



Current Opinion in Electrochemistry

journal homepage: www.elsevier.com

Single Molecule Insights into Interfacial Molecular Recognition for Model Electrochemical DNA Biosensors

Qufei Gu,^{1,2} Zachary Petrek,³ Rambod Rezayan,³ Tao Ye^{1,3,*}

¹Materials and Biomaterials Science and Engineering, University of California, Merced, California, 95343, United States

²Department of Plant Biology, Carnegie Institution for Science, Stanford, California, 94305, United States

³Department of Chemistry and Biochemistry, University of California, Merced, California, 95343, United States

Abstract

Electrochemical sensors that use surface-immobilized DNA to bind analytes and transduce the binding into electrochemical signals, have the potential for rapid, specific, and sensitive detection of bioanalytes via a compact and portable platform. However, accessing the structure of these surfaces/interfaces at the relevant spatial scale (< 10 nm), which determines the interfacial interactions and ultimately sensing performance, remains an unsolved challenge. Here, we review studies that have used high resolution atomic force microscope imaging and spatial statistical analysis tools to understand crowding interactions between thiolated DNA probes immobilized on gold electrodes and how such interactions impact target binding. We also review related studies that attempt to control the nanoscale spatial arrangement of the immobilized recognition elements to optimize sensing performance. These efforts have led to new advances in understanding of the structure-function relationships of DNA-based electrochemical biosensors to move the field toward rational engineering of these biosensing interfaces.

© 2017 Elsevier Inc. All rights reserved.

Keywords: Electrochemical DNA Sensors; Single Molecules; Atomic Force Microscopy; DNA Probes; Electrode Surfaces.

Introduction.

Compact, portable biosensors that can rapidly detect biomarkers in complex biological fluids without lengthy sample preparation steps, specialized personnel or facility have potentially transformative impacts on personalized medicine,[1] early diagnosis of debilitating illnesses,[2-4] as well as the containment of pandemics.[5] These surface-based biosensors typically immobilize the recognition element, molecules that bind or react with the biomarker of interest (target molecule) onto a material that transduces the recognition event into signals.[2-4] Since the invention of the electrochemical glucose biosensor,[1] electrochemistry has been a highly appealing signal transduction mechanism as electrochemical signals can be detected using compact devices with high sensitivity and selectivity.[6] One of the most widely used recognition elements is deoxyribonucleic acids (DNAs), due to their ease of preparation, high chemical stability, and ability to recognize a broad range of targets, from nucleic acids,[6] ions,[7] proteins[8, 9] to small molecules.[10, 11] At the interface between the solution and the transducer material, the capture DNA probes,

Please cite this article as: First author et al., Article title, Computer Vision and Image Understanding (2017), http://dx.doi.org/10.1016/j.cviu.2017.00.000

and the target molecules, experience interactions that differ markedly from their counterparts in dilute solutions.[12-19] Thus, a long-standing challenge with these electrochemical DNA sensors and other surface-based biosensors is such interactions may influence device performance characteristics in ways that are difficult to understand and predict,[20] leading to devices with suboptimal performance and reproducibility. A root cause of the challenge is that the structure of these surfaces/interfaces at the relevant spatial scale (10 nm and below), which fundamentally determines interfacial interactions, is largely inaccessible with the ensemble averaging techniques that have been commonly used to characterize these biosensors.[21] Due to the lack of knowledge in this key aspect of interfacial structure, it has also been largely unclear how different protocols to immobilize the recognition element on the transducer material influence the interfacial structures, and how such structures in turn influence interfacial interactions and ultimately device performance. This review focuses on questions on structure-function relationships concerning DNA based electrochemical biosensors. We will review new insights derived from single molecule studies of DNA monolayers on gold, which are model surfaces widely used in electrochemical DNA sensors [10, 11, 22, 23].

Surface immobilization of DNA onto a gold electrode.

Electrochemical DNA biosensors require the immobilization of the DNA probes onto a conductive solid support, such as ITO, carbon, conducting polymers, and gold, to transduce the binding to electrochemical signals.[6] These supports could be flat surfaces[6] or nanostructured materials.[24] While the DNA probes can be immobilized through nonspecific adsorption, covalent end tethering is more commonly used due to the high stability and control of probe orientation. Covalent end tethering can be realized by either covalent coupling of chemically modified probes to a surface with reactive functional groups[25] or attachment of thiolated probes to gold surface via Au-S bonds.[16] To avoid overcrowding the surface with DNA probes and reduce nonspecific interactions, the gold electrode is typically co-immobilized with another spacer thiol, such as 6-mercapto-1-hexanol.[16] This co-immobilization can be performed by simultaneous exposure of a solution containing the thiolated DNA and alkanethiol to the surface ("co-adsorption") or by sequential exposure, first to the thiolated DNA probe then to the alkanethiol ("backfilling", Figure 1A). To further disperse the DNA probes, the surface with pre-assembled alkanethiol SAM can be exposed to thiolated DNA probes ("insertion", Figure 1B).

In situ microscopy techniques revealed DNA SAMs may be more heterogeneous than assumed.

Electrochemical, spectroscopic, and microscopic techniques are the most common methods used for characterization of surfaces for electrochemical DNA sensors. Electrochemical techniques, including cyclic voltammetry, differential pulse voltammetry, square-wave voltammetry, and chronocoulometry, measure the electron transfer between the electroactive species and the electrode surface.[6] Hence these techniques can serve as mechanisms for signal transduction in biosensing. In addition to quantification of sensor performances, some of the techniques can provide information about the quality/density of the DNA SAM.[17, 21] These electrochemical techniques are complemented by spectroscopic methods that can provide valuable information about the biomolecules' orientation and the interface's composition, such as infrared spectroscopy,[20] surface enhanced Raman scattering,[26] X-ray photoelectron spectroscopy,[16] surface plasmon resonance.[14] While these ensemble averaging techniques are widely used in biointerface characterization, a limitation is the relative insensitivity to heterogeneity in local densities, binding affinities, and binding kinetics.

Although it was assumed that these DNA monolayers are largely homogeneous, [16] fluorescence microscopy studies of surface immobilized DNA on a gold electrode have revealed heterogeneity in probe density and molecular conformation even at the micron scale. [21] However, the gold electrode is incompatible with microscopy configurations that are conducive to single molecule imaging, such as total internal reflection fluorescence microscopy (TIRF). [27] Even if single molecule fluorescence imaging were feasible on these metal electrodes, the spatial resolution of super-resolution fluorescence microscopy, ~20 nm, [28] remains insufficient to characterize interacting DNA probes. Atomic force microscopy (AFM) appears ideally suited for this task due to its nanometer lateral resolution and *in situ* operation. [29] However, single DNA molecules on a biosensor surface are typically too immobile to be resolved by AFM[30, 31] because the surface is typically passivated with inert molecules that inhibit nonspecific adsorption. [23] To satisfy the contradictory requirements for facile target binding and high-resolution

AFM imaging, Ye and coworkers tethered DNA probes to surfaces that switch tethered DNA molecules between a pinned state that enables high resolution AFM imaging and a free state that allows for facile molecular recognition (Figure 2),[30-33] To minimize the impact of compositional (defect density) and uncontrolled morphological (surface roughness) heterogeneities and thus facilitate high resolution AFM imaging, they employed a highly ordered SAM on an Au(111) electrode to serve as a model for electrochemical DNA sensors.[33] This approach enabled Josephs et al. to carry out a systematic study of the spatial distribution of DNA end-tethered to 1-mercapto-6-hexanol passivated gold electrodes. [31] A surprising discovery is the extent of nanometer scale heterogeneity in surfaces that are prepared using prevalent methods, namely co-adsorption and backfilling (left panel of Figure 1A). The former refers to the simultaneous exposure of thiolated oligonucleotide and spacer thiol molecules to the electrode surface, while the latter includes a sequential deposition of thiolated oligonucleotide, followed by dilution with spacer thiol molecules whose own Au-S interactions will displace non-specifically adsorbed ssDNA. AFM imaging provided direct evidence for nanoscale phase segregation of the spacer molecules to the regions of high and low densities of DNA molecules (right panel of Figure 1A), rather than a uniformly distributed and appropriately diluted DNA SAM that had previously been assumed. Phase segregation has been routinely observed in many other multicomponent SAMs.[34] Due to the lateral mobility of thiolated DNA molecules when the surface is not yet packed with thiols, the molecules can diffuse laterally to assume the segregated state, which lowers the free energy. Such clustering/phase segregation of DNA probes may not be ideal for target binding and signal transduction.[8] Real space imaging also shows that the insertion method, which exposes a pre-assembled alkanethiol monolayer to a thiolated oligonucleotide solution (Figure 1B), immobilizes the probe molecules in a more random spatial distribution (right panel of Figure 1B). The protrusions were attributed to single DNA molecules pinned down to the SAMs.[30, 31] However, as the preformed SAM reduces the number of DNA molecules that are immobilized, the insertion approach may not be ideal for sensors that require the highest probe density.

The coordinates of individual probe molecules have made it possible to characterize the spatial distribution of these single molecules in a quantitative manner and provide insights that are not readily available through simple visual inspection of the microscopy images (Figure 3).[31, 33] A map of the nearest neighbour distances (NNDs) can visualize the interactions from nearest neighbours and reveal heterogeneity (Figure 3B). Even if the probes are randomly distributed, histograms revealed a broad distribution of NNDs due to the largely random nature of probe distribution. The comparison of the experimentally measured NNDs and those estimated based on the overall probe density suggests that the crowding interactions are more important than expected. Existing studies typically used the overall probe density to estimate the average distance of probes, $(A/n)^{1/2}$, where A is the area of the surface and n is the number of molecules.[15, 20] However, this distance is based on the assumption that the molecules are arranged in a square lattice. Histograms of measured NNDs shows that this quantity overestimates the mean NND by ~100% even if the surface is relatively uniform.[31, 33] Moreover, NND histograms showed 90% of probe molecules have NNDs less than the nominal average separation. Due to the largely random nature of spatial distribution, even if the overall probe density is low, there remains a fraction of probes that are close enough to interact. Nearest neighbours are not the only molecules responsible for the crowding interactions that are experienced by individual DNA probes. To examine the crowding by other molecules, we introduced a crowding function N_i(d) and related metric for nanoscale DNA probe crowding known as the "local crowding index" (LCI) to account for other molecules that might be close enough to interact with the probe molecule of interest. N_i(d) represents the number of molecules within a distance of d for a specific probe molecule with an index of i. The crowding distribution N(d, n) is the total number of DNA molecules that have n other molecules within a distance of d. Hence, a slice of the crowding distribution function diagram along d yields a histogram of n (Figure 3C). N(d, n) can be used to characterize DNA monolayers with a heterogeneous probe spatial distribution. For example, an MCH passivated DNA SAM, patches with high densities and those with low densities are often observed (Figure 3A).[21, 35] An area with a high-density region and a low-density region produces a bimodal histogram with two distinct populations in the crowding distribution function (Figure 3B). The LCI is defined as the crowding function or number of probes within the maximum distance across which crowding interactions could potentially affect probe-target interactions (Figure 3D).

Spatial distribution of DNA probes influences molecular recognition.

The aforementioned studies provide compelling evidence that the interactions between DNA probes are substantially more heterogeneous than commonly assumed. One possibility is that although there is a small fraction of probes that

are in close proximity, their roles in the overall target binding are negligible. Recent single molecule AFM studies of electrochemical DNA sensor surfaces (E-DNA) (Figure 4A) showed that these "outliers" may in fact be particularly important in target recognition.[33]

As shown in Figure 4B, the captured targets (worm-like protrusions) predominately appear in the areas where the probes are separated by about 10 nm at an intermediate probe density $(5.9 \times 10^{10} \, \text{probes/cm}^2)$. This effect is more pronounced at the lower target concentrations (Figure 4A) and shorter hybridization times (Figure 4B). In contrast, a homogenous target capture occurs where the probes are separated by $> 25 \, \text{nm}$ at a low probe density $(5.2 \times 10^9 \, \text{probes/cm}^2)$, right panel of Figure 2B). These results suggest that DNA hairpin probes having a neighbour that is 5-20 nm away more readily capture DNA targets. Our findings from single molecule imaging are in contrast with the assumption in studies based on ensemble averaging techniques: the crowding of DNA probes on the surface inhibits target binding due to steric hindrance and electrostatic repulsion.[33, 36] While the underlying mechanism remains to be fully elucidated, the unexpected cooperative effect between DNA hairpin probes, which accelerates the hybridization kinetics by at least an order of magnitude, can explain why these outliers, *i.e.*, closely spaced probes, may be a predominant contributor to target binding under specific circumstances. In contrast, on a biosensor surface where anti-cooperative effect is dominant, contributions from these outliers can be neglected as the target binding is inhibited within domains of clustered probes.

The link between probe spatial distribution and macroscopic properties of the biosensor is further illustrated in differences in binding kinetics of two DNA SAMs with similar probe densities.[36] Small outliers of clustered probes within heterogeneous spatial distributions of probes have illustrated a disproportionately large role in binding kinetics (Figure 5). The surface with a higher LCI and lower NND (7.66 × 10¹⁰ probes/cm²) showed faster hybridization kinetics compared to the biosensor with lower LCI and higher NND (8.25 × 10¹⁰ probes/cm²), despite similar surface densities. Characterizing these heterogeneous regions in terms of LCI and NND highlight the cooperative nature of E-DNA sensors under certain circumstances and can be used to numerically model the hybridization kinetics of the E-DNA sensor and potentially the overall performance.[36] Given that the kinetics of molecular recognition is a key determinant of the figures-of-merit of biosensors, including sensitivity, limit of detection, and detection time, designing biosensor surfaces that increase fraction of probes with the desired probe separation may help improve the performance.

Emerging surface immobilization methods can tailor the spatial patterns of DNA probes.

While the separation between probe molecules is a crucial factor in molecular recognition of target molecules, existing methods to immobilized DNA probes on electrode surfaces, such as backfilling, co-adsorption, and insertion, do not offer direct control over the inter-probe separation. Methods that offer more direct control over this important quantity to rationally engineer biosensor surfaces have emerged. Pei et al. used nanoscale DNA tetrahedra loaded with capture probes to regulate the inter-probe separation (Figure 6A).[8] It was proposed that the footprint of the tetrahedral structures helps maintain uniform inter-probe separations and facilitate probe-target recognition. They found that the attachment of probes to nanoscale DNA tetrahedra increased the target binding, improving the limit of detection (1 pM) by 250-fold in ssDNA target systems and 1000-fold (100 pM) in thrombin binding systems. Liu et al. immobilized DNA aptamer probes on gold surfaces in a folded, target bound state. [37] They hypothesized that immobilizing probes in this manner would ensure inter-probe separations that allow the DNA aptamer strands to more readily undergo the conformational change necessary for target capture (Figure 6B). Their approach resulted in significant improvement in the signal gain as well as limit of detection. To further control the inter-probe spacing, Gu et al. deposited DNA origami tiles possessing a pair of thiolated DNA capture probes with a predesigned separation distance onto a SAM coated electrode surface and denatured DNA origami frame to expose the spatial pattern (DNA origami lithography in Figure 6C),[38] Spatial statistical analysis of AFM images revealed the probe molecule transfer yield to be 70%, comparable to the highest yield achieved with DNA nanostructure-mediated nanoimprinting methods. This approach, which is compatible with high resolution AFM and in principle offers greater control over the inter-probe separation, may offer a pathway toward single molecule patterns to systematically explore the structure-function relationship of interfacial molecular recognition.

Perspective.

Due to the limited fundamental understanding of interfaces used in electrochemical biosensors, currently the engineering of these biosensors remains has been more of art than of science. The development of AFM imaging techniques to map single probe molecules on model sensor surfaces and a spatial statistical framework has offered a new window into how the interfacial environment is altering how the DNA probes recognize target molecules. This single molecule approach can be potentially extended to other surface-based electrochemical biosensors, such as aptamer-based biosensors.[11, 37] Hence a molecular level understanding of interfacial molecular recognition and signal transduction may begin to emerge for these electrochemical biosensors. Such mechanistic understandings of sensors based on flat surfaces may serve as a starting point to understand structure-function relationship of biosensors based on nanomaterials.[24] Moreover, by coupling these mechanistic understanding with new surface immobilization methods that offer direct control of the spatial patterns of probe molecules, it may be possible to rationally tailor the biosensor surfaces to produce electrochemical biosensors with improved performance.

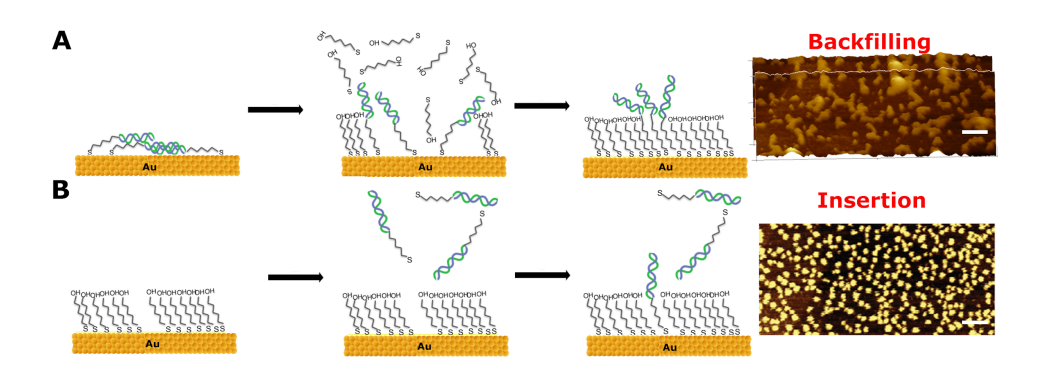


Figure 1. Thiolated DNA monolayers prepared by (A) backfilling double-stranded DNA (dsDNA) with MCH (6-mercapto-1-hexanol)[16] and by (B) inserting DNA probes into preassembled MCH self-assembled monolayer (SAM). The scale bars are 100 nm. Reproduced with permission.[31] Copyright 2013, American Chemical Society.

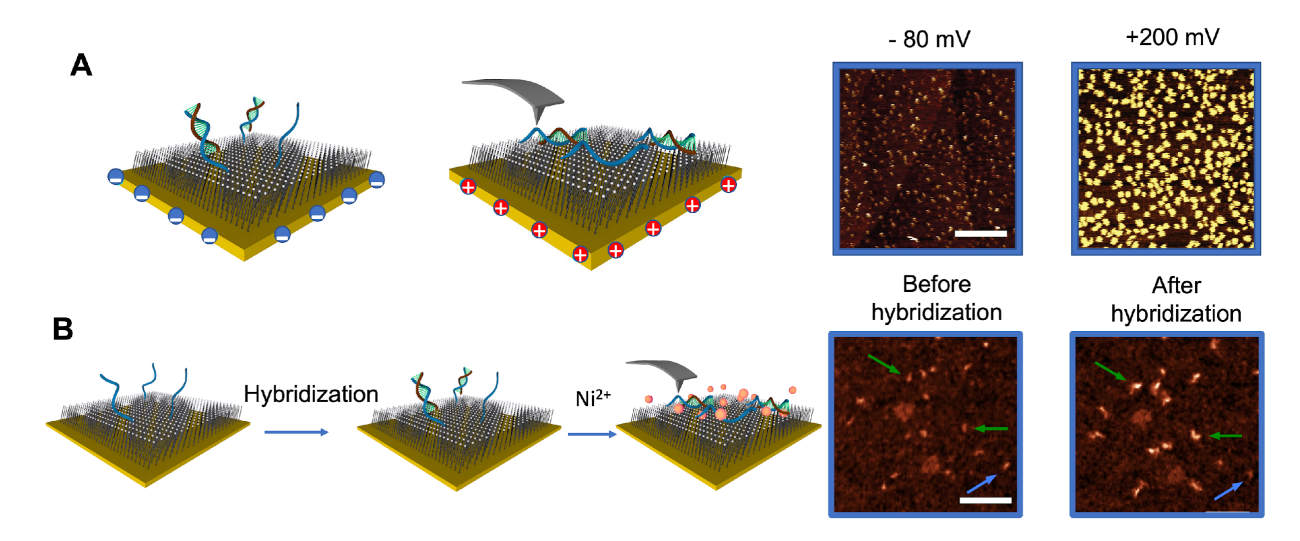


Figure 2. Single-molecule atomic force microscopy (AFM) characterization of surface-immobilized DNAs. (A) AFM imaging of DNA monolayer prepared by inserting thiolated DNA to a SAM of 6-mercapto-1-hexanol and imaged under different electrode potentials. When the potential is above the potential of zero charge, the positive surface charges pin DNA molecules to the surface and allow them to be imaged as protrusions as high as 2 nm. Scale bar is 100 nm. Reproduced with permission.[39] Copyright 2012, American Chemical Society (B) AFM imaging of DNA monolayer prepared by insertion of thiolated DNA molecules into preassembled 11-mercaptoundecanoic acid (MUDA) SAM. Hybridization is carried out in a monovalent cation buffer in which the DNA probes experience reduced interactions with the surface and AFM imaging is carried out in a divalent cation buffer that pins the DNA to the carboxyl terminated surface. Scale bar is 50 nm. Reproduced with permission.[32] Copyright 2013, American Chemical Society.

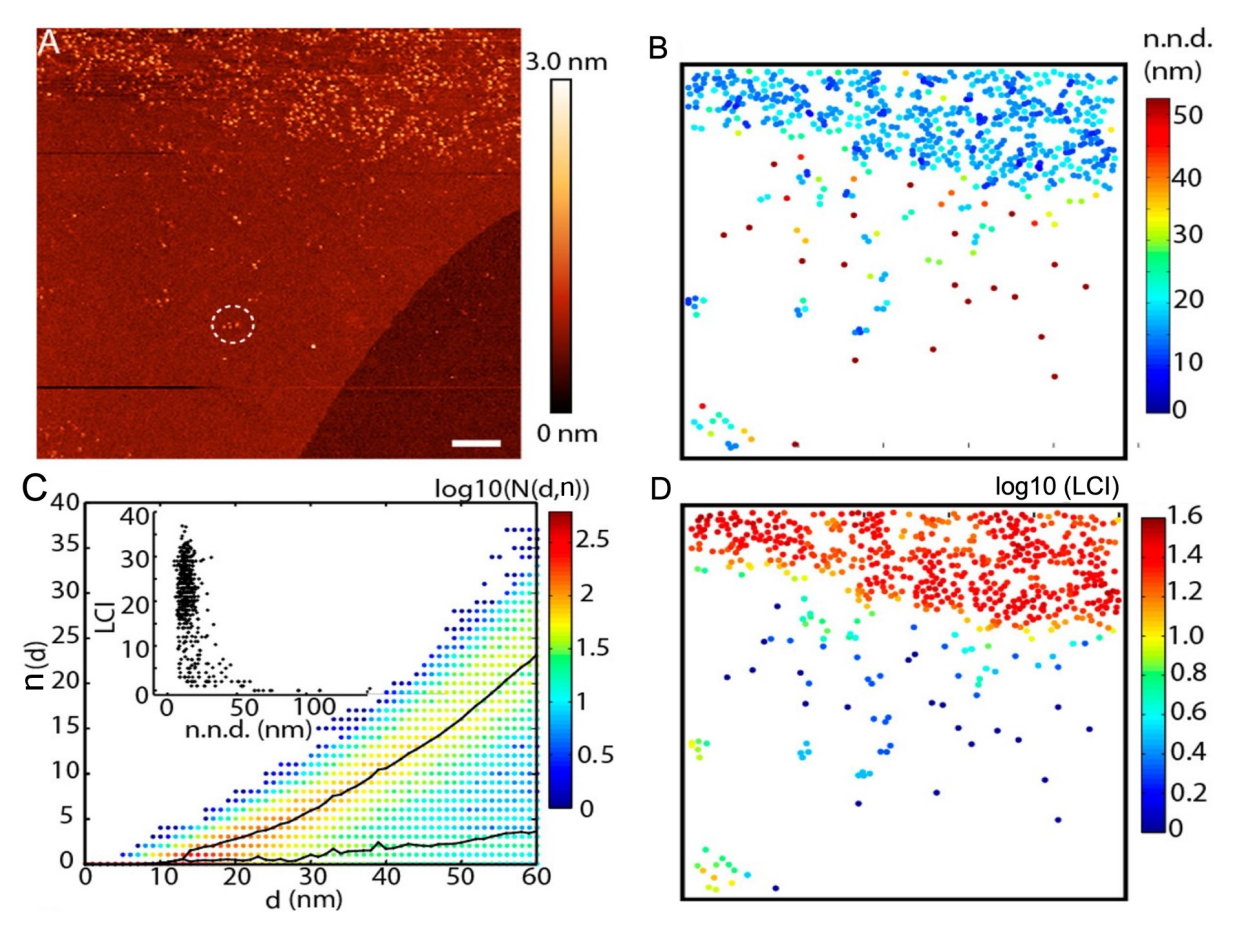


Figure 3. (A) Tapping mode AFM image of thiolated DNA inserted into MCH SAM where two populations (high density and low density) are apparent. The dashed white circle highlights a low-density region of probes with nearest-neighbor distances similar to those in the high-density regions. (B) nearest-neighbor distance graphed at the respective locations of the probes from (A). (C) Histogram of the crowding distribution function N(d,n) for the surface in (A). Lines with dots are the means from fitting the N(d,n) at each d as the mixture of two Gaussian distributions. (Inset) Plot of N(60 nm) vs n.n.d. for each DNA molecule shows that DNA molecules in both the high-density and low-density regions may have similar nearest-neighbor distances despite large differences in local density. (D) Local crowding index, defined here as N(60 nm) (see main text). Reproduced with permission.[31] Copyright 2013, American Chemical Society.

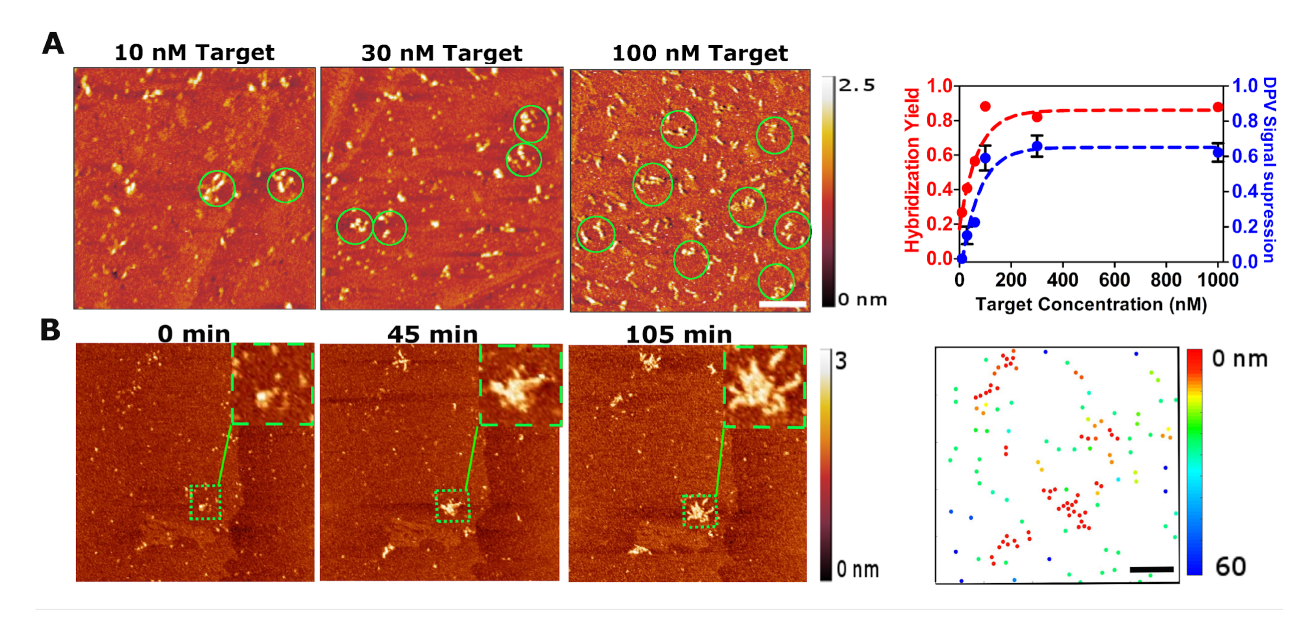


Figure 4. (A) Representative AFM images of DNA modified electrode surfaces exposed to complementary target DNAs at 10, 30 and 100 nM. Probe-target complexes tend to form clusters (highlighted by green circles). The relation between DPV signal suppression (blue curve) and hybridization yield (red curve) at different target concentrations (right panel). Differential pulse voltammetry (DPV) applies a series of amplitude potential pulses superimposed on the linear potential sweep. The current is then measured immediately before and after each potential change. The scale bar is 100 nm. (B) Time evolution of heterogeneous spatial distributions of DNA surface hybridization. Representative AFM images of DNA modified electrode surfaces after exposed to 10 nM target DNA for 0, 45 and 105 min. Analyzing spatial patterns using the nearest-neighbor distance (NND) of probes measured from AFM images. The color bar indicates the range of NND from 0 nm (red) to 60 nm (blue). Scale bar is 100 nm. Reproduced with permission.[33] Copyright 2018, American Chemical Society.

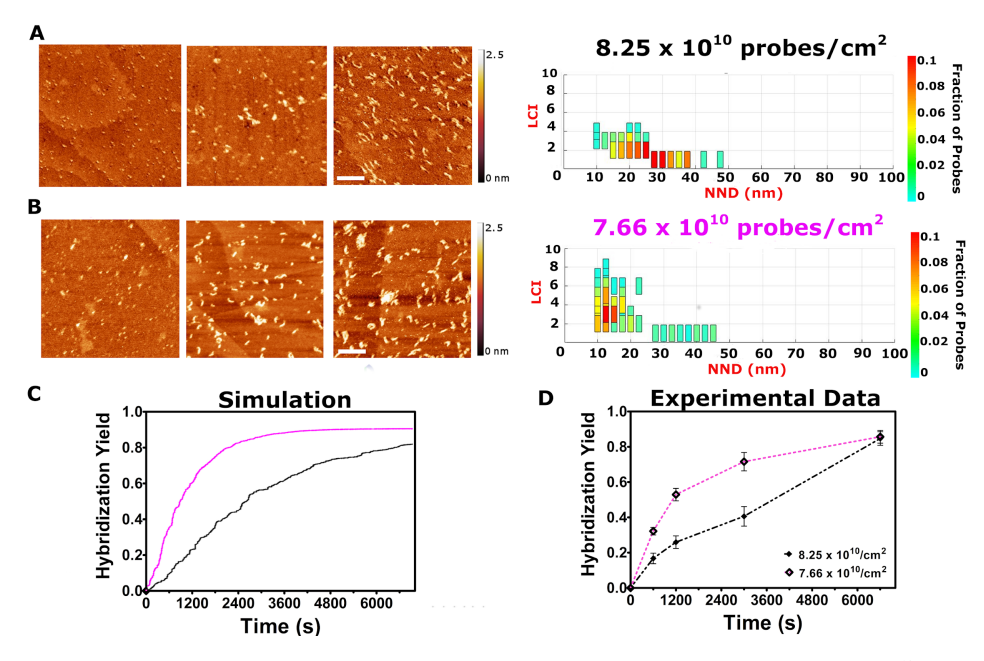


Figure 5. Representative AFM images of DNA modified electrode surfaces with similar probe densities ((A) 8.25×10^{10} and (B)7.66 x 10^{10} DNA probes/cm²) but different probe spatial organizations. Spatial arrangements of DNA probes as a function of both LCI and NND (right panel in Figure A and B). The color bar indicates the range of fractions of probes. Scale bar is 100 nm. (C) Numerical simulations of the hybridization kinetics of DNA modified electrode surfaces at 8.25×10^{10} (black solid line) and 7.66×10^{10} (purple solid line) DNA probes/cm². (D) Experimentally derived hybridization kinetics at 8.25×10^{10} (black dash line) and 7.66×10^{10} (purple dash line) DNA probes/cm². Reproduced with permission.[36] Copyright 2021, American Chemical Society.

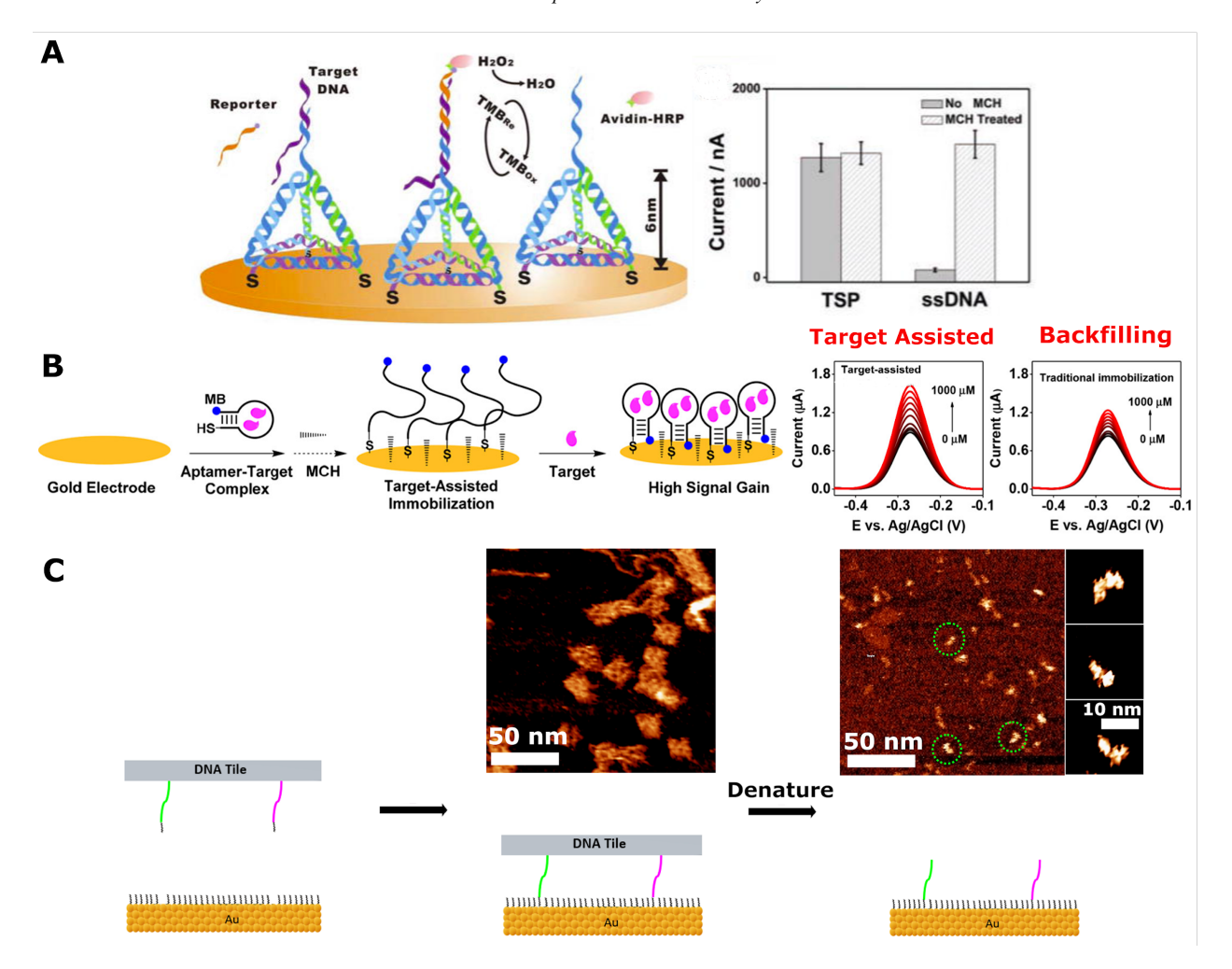


Figure 6. (A) Using the footprint of a DNA nanostructure to control inter-probe separation. This DNA nanostructure tethered to the electrode surface through three thiols at the base of the "pyramid", leaving a free-standing probe at the top. The TSP (tetrahedron-structured probe) carrier was assembled from three thiolated DNA fragments and one DNA fragment carrying the probe sequence. Comparison of ssDNA and TSP probebased sensor performance with or without MCH passivation. Reproduced with permission.[8] Copyright 2010, Wiley. (B) Modification of an electrode surface using target-assisted immobilization strategy. Square-wave voltammetry (SWV) spectra of electrodes modified with the aptamer—target complex or aptamer alone. Reproduced with permission.[37] Copyright 2021, American Chemical Society. (C) DNA mini-tile carrying a pair of thiolated staples with an extension protruding from the origami surface (green and purple) is deposited onto a MUDA SAM-coated Au(111) electrode surface. Representative AFM image of DNA minitiles before and after denaturation. The figures on the right are zoom-in images of the highlighted staples (green circle). Reproduced with permission.[38] Copyright 2021, American Chemical Society.

Author contributions

Q.G. and R.R. prepared figures, all authors contributed to the writing of this manuscript.

Declaration of competing interest

There are no conflicts to declare.

Acknowledgements

The authors acknowledge support by the National Science Foundation (CHE-1808213) and the Department of Energy (DE-SC0020961).

References

- [1] Wang J. Electrochemical glucose biosensors. Chemical Reviews. 2008;108:814-25.
- [2] Kelley SO. Advancing ultrasensitive molecular and cellular analysis methods to speed and simplify the diagnosis of disease. Accounts Chem Res. 2017;50:503-7.
- [3] Xi Q, Zhou DM, Kan YY, Ge J, Wu ZK, Yu RQ, et al. Highly sensitive and selective strategy for microrna detection based on ws2 nanosheet mediated fluorescence quenching and duplex-specific nuclease signal amplification. Anal Chem. 2014;86:1361-5.
- [4] Thomas JM, Chakraborty B, Sen D, Yu HZ. Analyte-driven switching of DNA charge transport: De novo creation of electronic sensors for an early lung cancer biomarker. J Am Chem Soc. 2012;134:13823-33.
- [5] Feng W, Newbigging AM, Le C, Pang B, Peng H, Cao Y, et al. Molecular diagnosis of covid-19: Challenges and research needs. Anal Chem. 2020;92:10196-209.
- [6]* Drummond TG, Hill MG, Barton JK. Electrochemical DNA sensors. Nat Biotechnol. 2003;21:1192-9.
- *An influential early review article on electrochemical DNA sensors.
- [7] McGhee CE, Loh KY, Lu Y. Dnazyme sensors for detection of metal ions in the environment and imaging them in living cells. Curr Opin Biotech. 2017;45:191-201.
- [8]* Pei H, Lu N, Wen YL, Song SP, Liu Y, Yan H, et al. A DNA nanostructure-based biomolecular probe carrier platform for electrochemical biosensing. Advanced Materials. 2010;22:4754-+.
- *A study showing how DNA nanostructures can be used to regulate spacing between DNA probes and improve sensing performance.
- [9] Xiao Y, Piorek BD, Plaxco KW, Heeger AJ. A reagentless signal-on architecture for electronic, aptamer-based sensors via target-induced strand displacement. Journal of the American Chemical Society. 2005;127:17990-1.
- [10] Swensen JS, Xiao Y, Ferguson BS, Lubin AA, Lai RY, Heeger AJ, et al. Continuous, real-time monitoring of cocaine in undiluted blood serum via a microfluidic, electrochemical aptamer-based sensor. Journal of the American Chemical Society. 2009;131:4262-6.
- [11] Ploense KL, Dauphin-Ducharme P, Arroyo-Curras N, Williams S, Schwarz N, Kippin T, et al. Real-time pharmacokinetic and pharmacodynamic measurements of drugs within the brains of freely behaving rats. Faseb J. 2020:34.
- [12] Cederquist KB, Golightly RS, Keating CD. Molecular beacon-metal nanowire interface: Effect of probe sequence and surface coverage on sensor performance. Langmuir. 2008;24:9162-71.
- [13] Cederquist KB, Keating CD. Hybridization efficiency of molecular beacons bound to gold nanowires: Effect of surface coverage and target length. Langmuir. 2010;26:18273-80.
- [14] Peterson AW, Heaton RJ, Georgiadis RM. The effect of surface probe density on DNA hybridization. Nucleic Acids Res. 2001:29:5163-8.
- [15] Ricci F, Lai RY, Heeger AJ, Plaxco KW, Sumner JJ. Effect of molecular crowding on the response of an electrochemical DNA sensor. Langmuir. 2007;23:6827-34.
- * A study that used classical electrochemical techniques to investigate the crowding effect on DNA sensors.
- [16] Herne TM, Tarlov MJ. Characterization of DNA probes immobilized on gold surfaces. Journal of the American Chemical Society. 1997;119:8916-20.
- * A study that pioneered DNA SAMs that have been used in many electrochemical biosensors.

- [17] Steel AB, Herne TM, Tarlov MJ. Electrochemical quantitation of DNA immobilized on gold. Analytical Chemistry. 1998;70:4670-7.
- [18] Xu F, Pellino AM, Knoll W. Electrostatic repulsion and steric hindrance effects of surface probe density on deoxyribonucleic acid (DNA)/peptide nucleic acid (pna) hybridization. Thin Solid Films. 2008;516:8634-9.
- [19] Johnson-Buck A, Nangreave J, Jiang S, Yan H, Walter NG. Multifactorial modulation of binding and dissociation kinetics on two-dimensional DNA nanostructures. Nano Lett. 2013;13:2754-9.
- [20]* Rao AN, Grainger DW. Biophysical properties of nucleic acids at surfaces relevant to microarray performance. Biomater Sci-Uk. 2014;2:436-71.
- *A comprehensive review article on the properties of surface immobilized DNA.
- [21]** Bizzotto D, Burgess IJ, Doneux T, Sagara T, Yu HZ. Beyond simple cartoons: Challenges in characterizing electrochemical biosensor interfaces. ACS Sens. 2018;3:5-12.
- **An insightful review article on challenges toward molecular level understanding of electrochemical biosensor interfaces.
- [22] Petrovykh DY, Kimura-Suda H, Whitman LJ, Tarlov MJ. Quantitative analysis and characterization of DNA immobilized on gold. J Am Chem Soc. 2003;125:5219-26.
- [23] Ricci F, Zari N, Caprio F, Recine S, Amine A, Moscone D, et al. Surface chemistry effects on the performance of an electrochemical DNA sensor. Bioelectrochemistry. 2009;76:208-13.
- [24] Kelley SO, Mirkin CA, Walt DR, Ismagilov RF, Toner M, Sargent EH. Advancing the speed, sensitivity and accuracy of biomolecular detection using multi-length-scale engineering. Nat Nanotechnol. 2014;9:969-80.
- [25] Nakamura F, Ito E, Hayashi T, Hara M. Fabrication of cooh-terminated self-assembled monolayers for DNA sensors. Colloid Surface A. 2006;284:495-8.
- [26] Papadopoulou E, Gale N, Thompson JF, Fleming TA, Brown T, Bartlett PN. Specifically horizontally tethered DNA probes on au surfaces allow labelled and label-free DNA detection using sers and electrochemically driven melting. Chem Sci. 2016;7:386-93.
- [27] Monserud JH, Schwartz DK. Mechanisms of surface-mediated DNA hybridization. ACS Nano. 2014;8:4488-99
- [28] Schermelleh L, Ferrand A, Huser T, Eggeling C, Sauer M, Biehlmaier O, et al. Super-resolution microscopy demystified. Nat Cell Biol. 2019;21:72-84.
- [29] Kodera N, Yamamoto D, Ishikawa R, Ando T. Video imaging of walking myosin v by high-speed atomic force microscopy. Nature. 2010;468:72-+.
- [30] Josephs EA, Ye T. A single-molecule view of conformational switching of DNA tethered to a gold electrode. Journal of the American Chemical Society. 2012;134:10021-30.
- [31]* Josephs EA, Ye T. Nanoscale spatial distribution of thiolated DNA on model nucleic acid sensor surfaces. ACS Nano. 2013;7:3653-60.
- * Introduced a spatial statistical framework to analyze spatial distribution of DNA probes within DNA SAMs.
- [32] Abel GR, Jr., Josephs EA, Luong N, Ye T. A switchable surface enables visualization of single DNA hybridization events with atomic force microscopy. J Am Chem Soc. 2013;135:6399-402.
- [33]** Gu Q, Nanney W, Cao HH, Wang H, Ye T. Single molecule profiling of molecular recognition at a model electrochemical biosensor. J Am Chem Soc. 2018;140:14134-43.
- ** Discovery of cooperative effects of crowded DNA probes from the first study of single molecule AFM imaging of functioning electrochemical DNA sensor surface.
- [34] Smith RK, Lewis PA, Weiss PS. Patterning self-assembled monolayers. Prog Surf Sci. 2004;75:1-68.
- [35] Murphy JN, Cheng AKH, Yu HZ, Bizzotto D. On the nature of DNA self-assembled monolayers on au: Measuring surface heterogeneity with electrochemical in situ fluorescence microscopy. Journal of the American Chemical Society. 2009;131:4042-50.
- [36]** Gu Q, Cao HH, Zhang Y, Wang H, Petrek ZJ, Shi F, et al. Toward a quantitative relationship between nanoscale spatial organization and hybridization kinetics of surface immobilized hairpin DNA probes. ACS Sens. 2021.
- ** The first study showing the correlation between the spatial patterns of DNA probes and overall hybridization kinetics of DNA SAMs.
- [37]** Liu YZ, Canoura J, Alkhamis O, Xiao Y. Immobilization strategies for enhancing sensitivity of electrochemical aptamer-based sensors. ACS Appl Mater Inter. 2021;13:9491-9.

Current Opinion in Electrochemistry

- ** The introduction of a simple immoblization strategy that utilizes the footprint of target molecules bound to DNA aptamer probes to regulate the spatial arrangement of DNA aptamer probes on electrochemical biosensors. [38] Gu QF, Zhang YA, Cao HH, Ye ST, Ye T. Transfer of thiolated DNA staples from DNA origami nanostructures to self-assembled monolayer-passivated gold surfaces: Implications for interfacial molecular recognition. ACS Appl Nano Mater. 2021;4:8429-36.
- [39] Josephs EA, Ye T. Electric-field dependent conformations of single DNA molecules on a model biosensor surface. Nano Letters. 2012;12:5255-61.